

PcrA Helicase Tightly Couples ATP Hydrolysis to Unwinding Double-Stranded DNA, Modulated by the Initiator Protein for Plasmid Replication, RepD[†]

Andrew F. Slatter,[‡] Christopher D. Thomas,[§] and Martin R. Webb^{*‡}

[‡]MRC National Institute for Medical Research, The Ridgeway, Mill Hill, London NW7 1AA, U.K., and [§]Astbury Centre for Structural Molecular Biology, University of Leeds, Leeds LS2 9JT, U.K.

Received January 22, 2009; Revised Manuscript Received April 20, 2009

ABSTRACT: The plasmid replication initiator protein, RepD, greatly stimulates the ability of the DNA helicase, PcrA, to unwind plasmid lengths of DNA. Unwinding begins at *oriD*, the double-stranded origin of replication that RepD recognizes and covalently binds to initiate replication. Using a combination of plasmids containing *oriD* and oligonucleotide structures that mimic parts of *oriD*, the kinetics of DNA nicking and separation have been determined, along with the coupling ratio between base separation and ATP hydrolysis. At 30 °C, the rate of nicking is 1.0 s⁻¹, and translocation is ~30 bp s⁻¹. During translocation, the coupling ratio is one ATP hydrolyzed per base pair separated, the same as the value previously reported for ATP hydrolyzed per base moved by PcrA along single-stranded DNA. The data suggest that processivity is high, such that several thousand base-pair plasmids are unwound by a single molecule of PcrA. In the absence of RepD, a single PcrA is unable to separate even short lengths (10 to 40 bp) of double stranded DNA.

PcrA is a well-studied member of the superfamily 1 helicases. PcrA from *Bacillus stearothermophilus* binds to single-stranded DNA (ssDNA¹) and translocates at ~50 bases s⁻¹ at 20 °C, hydrolyzing one ATP per base movement (1). Its movement is from 3' to 5' along DNA, but with low processivity with double-stranded DNA (dsDNA) (2, 3). Structures of PcrA from *B. stearothermophilus* have been published that represent different states of the bound adenosine nucleotide (4–6). From these, it is apparent that monomeric PcrA translocates along ssDNA via a series of changes in base binding pockets, in turn associated with different nucleotide states of the ATP hydrolysis cycle.

On its own, PcrA is a poor helicase: it has difficulty separating even short lengths of duplex DNA (2, 3). Although it can translocate along ssDNA driven by ATP hydrolysis, it dissociates shortly after meeting a duplex section. Because of this, any section of partially separated, duplex DNA reanneals rapidly. This can be overcome *in vitro* by having several PcrA molecules bound to the same length of DNA (3, 7). PcrA requires a single-stranded DNA 3'-overhang to bind prior to any DNA unwinding (8). If this overhang is long enough, it can bind multiple PcrA

molecules. When these move along the DNA in the 3' to 5' direction into the duplex portion, dissociation of the first PcrA may allow the second to move into its place prior to reannealing. Alternatively, if the concentration of free PcrA is high, binding may be fast enough to limit any reannealing. In this way, the train of PcrA molecules can move through the duplex, in a way proposed for other helicases that otherwise would have low processivity (9, 10). PcrA from free solution can bind to the single strand at the rear of the train, thus propagating this effect. This binding and strand separation has very little or no sequence specificity.

In vivo PcrA is involved in asymmetric, rolling circle replication of plasmids of the pT181 family (11). Duplex separation occurs from a particular double-stranded origin of replication (dso), and the subsequent replication of the two ssDNA strands occurs sequentially by temporally and spatially independent processes. Leading strand synthesis is unidirectional from *ori* and follows the duplex separation around the plasmid. In contrast, the lagging strand synthesis is initiated from a separate single-stranded origin, which only becomes available once the duplex separation has gone past this origin (12). The plasmid dso sequence has several inverted complementary repeats (ICRs) involved in origin function, and therefore, there may be secondary structure in the DNA with short cruciforms extruded (13, 14). One of these inverted repeats, ICRII, contains the sequence that is nicked on one strand by the initiator protein, Rep, forming a covalent bond through a phosphotransfer reaction of the DNA 5'-phosphate to a tyrosine (Figure 1) (14, 15). This leaves the initiator protein attached at the 5'-end of the template for lagging strand synthesis. The cleavage is also thought to result in a short section of single-stranded DNA exposed on the opposing strand

[†]This work was supported by the Medical Research Council, U.K. (to A.F.S. and M.R.W.) and by The Wellcome Trust (062973 to C.D.T.).

*To whom correspondence should be addressed. Tel: (+44) 20 8816 2078. Fax: (+44) 20 8906 4477. E-mail: mwebb@nimr.mrc.ac.uk.

¹Abbreviations: ssDNA, single-stranded DNA; dsDNA, double-stranded DNA; dso, double-stranded origin of replication; SSB, single-stranded DNA binding protein from *Escherichia coli*; DCC-SSB, SSB (G26C) labeled with IDCC (*N*-[2-(iodoacetamido)ethyl]-7-diethylaminocoumarin-3-carboxamide); MDCC-PBP, phosphate binding protein (A197C) from *E. coli*, labeled with MDCC (*N*-[2-(1-maleimidyl)ethyl]-7-diethylaminocoumarin-3-carboxamide); ICR, inverted complementary repeat.

to the 3'-side of the RepD-DNA complex. An adjacent, inverted repeat in the *dso* sequence, ICRIII, provides specificity between particular Rep proteins and their correct plasmid substrate (16, 17). Once Rep is loaded at the *dso* sequence, the short single-stranded region is a potential substrate for PcrA binding. Thus, Rep enables PcrA to bind to the plasmid in the correct position for the latter to separate the duplex DNA ahead of replication. The presence of Rep enables the PcrA to separate the duplex with high processivity (2) but by a mechanism that has not yet been elucidated.

Here, we analyze the interaction of the three elements to produce plasmid unwinding: the initiator protein, RepD, and its partner *dso*, *oriD*, from *Staphylococcus aureus* plasmid pC221, together with PcrA from *B. stearothermophilus*. In order to address the roles of PcrA and RepD, translocation kinetics were measured using oligonucleotide models of the initiation region as well as complete plasmids. These have included measurements of ATP hydrolysis to determine the coupling between translocation and hydrolysis during unwinding. These data provide evidence for high processivity of PcrA in plasmid unwinding: one PcrA molecule is sufficient to unwind one plasmid without premature dissociation.

EXPERIMENTAL PROCEDURES

PcrA from *B. stearothermophilus* was prepared as described previously (8) with the exception that the PcrA pool from the heparin-Sepharose column was pure enough to use directly, as no additional bands were visible by SDS-PAGE gel analysis. PcrA was quantified using the extinction coefficient of $75875 \text{ M}^{-1} \text{ cm}^{-1}$ at 280 nm, calculated from the sequence (18). RepD from *Staphylococcus aureus* was prepared as described previously (17) with the following changes. After precipitation with ammonium sulfate, RepD was resuspended and applied to columns of Q-Sepharose (6 mL) and heparin-Sepharose (20 mL) (both from GE Healthcare) in series. The Q-Sepharose column was removed after loading, and elution of RepD from the heparin-Sepharose column was performed as described previously. DCC-SSB and MDCC-PBP were prepared as described previously (19–21).

Labeled and unlabeled oligonucleotides were purchased from Eurogentec (Southampton, U.K.). In order to make the DNA substrates, oligonucleotides were generally mixed at equimolar concentrations at either 50 or 100 μM in a volume of 50 or 100 μL , respectively, in a buffer containing 50 mM Tris·HCl at pH 7.5, 150 mM NaCl, and 3 mM MgCl_2 . Cy3- and Dabcyl-labeled oligonucleotides were mixed at a 5:6 molar ratio, in order to minimize free Cy3 (i.e., not paired and therefore quenched by Dabcyl). After mixing, oligonucleotides were heated to 95 °C for 5 min in a Biometra thermocycler, before cooling to room temperature for 2 h and were then stored frozen at –20 °C.

Heparin was purchased from Sigma and purified using NAP-25 (GE healthcare) columns to remove phosphate. Fractions were analyzed for phosphate content using fluorescence of the phosphate sensor, MDCC-PBP, and the heparin content was determined by titration with Azure A (22).

The 3094 bp plasmid, pCERoriD, has been described previously (2). Plasmids of different lengths were made, derived from pCERoriD. The 2437 bp plasmid was made by removing regions of unessential DNA by a strategy of restriction digestion followed by religation. Briefly, a 359 bp region was removed by double digest with *Hind*III and *Bsp*LU11I, followed by digestion with mung bean nuclease and blunt ended ligation to give a

plasmid of 2731 bp. An additional *Nde*I site was introduced to this using QuikChange II mutagenesis (Stratagene), followed by restriction digestion to remove a 294 bp region, and religation. The 3650 bp plasmid was made by inserting a 556 bp fragment, produced by *Nde*I digestion of lambda DNA, into pCERoriD, also digested with *Nde*I. The 4907 bp plasmid was made by inserting a 1829 bp fragment, produced by *Eco*RI and *Xma*CI digestion of lambda DNA, into pCERoriD also digested by *Eco*RI and *Xma*CI. The 6083 bp and 6639 bp plasmids were made by amplifying a 3015 bp fragment of lambda DNA by PCR using primers with the sequences CGGAATCCGGAGTAC-GAACGCCATCGACTTACGCG and CCCCCGGGGGCGCTGTCAT TAATCTGCA CACCGGC, containing restriction sites for *Eco*RI and *Ava*I, respectively. This fragment was digested with *Eco*RI and *Ava*I, and then ligated into the 3094 bp and 3650 bp plasmids, both digested with the same enzymes. All plasmids were transformed into *E. coli* DH5 α and prepared using miniprep or midiprep kits (Qiagen).

Anisotropy Titration Measurements. Fluorescence anisotropy titrations were performed at 30 °C using an ISS PC1 photon counting spectrofluorometer with a Xenon arc lamp. Anisotropy was calculated using the equations as described (23). Observed anisotropy data were fitted to obtain dissociation constants using GraFit fitting software (24).

Stopped-Flow Kinetics Measurements. All stopped-flow fluorescence measurements in this investigation were performed at 30 °C using a Hi-Tech stopped-flow apparatus with a xenon-mercury lamp (TgK Scientific, U.K.). Solution conditions and wavelengths for individual measurements are given in the figure legends. In all stopped-flow measurements described here, the stated concentrations are those in the mixing chamber unless shown otherwise. Anisotropy was measured with the instrument in the T format, allowing simultaneous acquisition of parallel (I_{\parallel}) and perpendicular (I_{\perp}) components. This enabled anisotropy, $(I_{\parallel} - I_{\perp})/(I_{\parallel} + 2I_{\perp})$, and intensity $(I_{\parallel} + 2I_{\perp})$ to be calculated from the same reaction profile (25). Traces shown in figures are the average of 2–4 acquisitions using the same experimental solutions, except Figures 7 and 8, which are single traces. All measurements were repeated with different solutions.

RESULTS

Design of DNA Substrates. Initiation of plasmid replication requires the formation and translocation of a specific complex of RepD, DNA, and PcrA. To study these processes in real time and determine the extent of formation, signals are required that monitor each step. Partial duplex oligonucleotide substrates provide useful tools for investigating both complex formation and initial DNA unwinding. The DNA substrates used in this investigation are shown in Figure 2 and were designed to mimic the preunwinding complex, once loaded with RepD and PcrA (Figure 1). Sections of the *oriD* sequence elements, ICRII and ICRIII, were included within the sequences. These DNA substrates have been labeled with fluorophores in various ways to measure RepD and PcrA binding, RepD nicking, and duplex separation; these are described below. In some cases, the illustrated oligonucleotides are parent members of a series with different lengths of duplex.

RepD and PcrA Binding to Partial Duplex DNA Substrates. In order to obtain optimal conditions for measuring translocation, it was necessary to investigate both the affinities of various components that form the initiation complex and to get

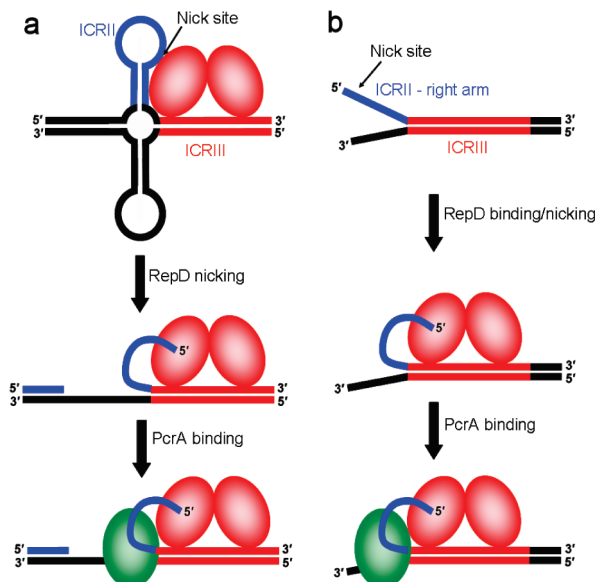


FIGURE 1: Cartoon of initiation of replication by RepD and PcrA at the *oriD* site. The mode of RepD binding is not known and therefore is shown diagrammatically. (a) RepD nicking and PcrA loading to form the initiation complex. (b) Illustration of the oligonucleotide model substrate.

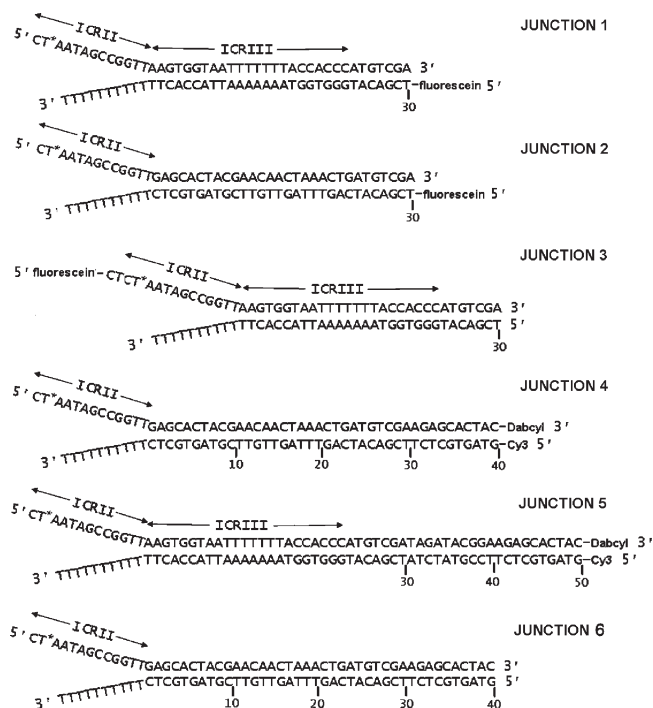


FIGURE 2: Representative oligonucleotide junctions used in this work. The asterisk indicates the cleavage position. In some case junctions with different lengths, duplex sections were used. These duplexes were shortened at the downstream (right) end of the duplex sequences shown, to give the appropriate duplex length as indicated.

an idea of the time-scale of formation. In this way, conditions were found that lead to complete formation of the initiation complex.

Fluorescence anisotropy was used to detect binding of RepD and PcrA to a partial duplex DNA substrate, containing the right arm of ICRII and the duplex ICRIII sequence and a fluorescein at the end of the ICRIII duplex (Junction 1 in Figure 2). Upon addition of RepD to the DNA, the anisotropy increases

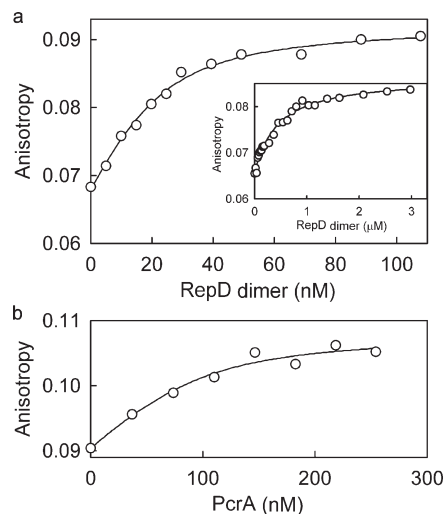


FIGURE 3: Fluorescence anisotropy titrations, following the formation of the RepD-DNA·PcrA complex. Measurements were made at 30 °C in buffer containing 50 mM Tris·HCl at pH 7.5, 200 mM KCl, 10 mM MgCl₂, 1 mM EDTA, and 10% ethanediol, exciting with vertically polarized light at 497 nm, and emission measured using a 515 nm cut off filter. (a) Titration of RepD into 20 nM Junction 1 (Figure 2) gives an apparent dissociation constant of 6 nM. This constant increases to 379 nM, when ICRIII is removed from the duplex (Junction 2) (inset, DNA concentration is 50 nM). (b) Addition of PcrA to a preformed complex of RepD-DNA (+ICRIII, Junction 1), from 100 nM DNA and 440 nM RepD, gives a K_d of 22 nM.

(Figure 3a). Anisotropy is dependent on the rotational correlation time of the fluorophore, which is often dependent on the molecular mass of its complex, thus increasing as RepD binds to the DNA. A titration of RepD into a solution of Junction 1 (DNA is defined in Figure 2) is shown in Figure 3a. This gives the range of concentrations required to bind RepD to this DNA quantitatively, although this measurement does not distinguish between binding and covalent linkage. For convenience, the data were fitted for reversible binding and give an apparent equilibrium constant, K_{app} , of 6 nM. This value represents an overall approximate assessment of affinity: the limited sensitivity of the method requires a relatively high concentration of fluorescent junction, but this approximation is sufficient for the main purpose of determining suitable conditions for subsequent kinetic measurements. If a similar oligonucleotide junction is used that does not contain ICRIII (Junction 2 in Figure 2), much weaker binding is observed with a K_{app} of 379 nM (inset Figure 3a).

Addition of PcrA to a preformed complex of RepD and Junction 1 DNA, which includes the ICRIII duplex sequence, causes a further increase in anisotropy (Figure 3b), indicating that PcrA is binding to the RepD-DNA complex with a K_d of 22 nM. This junction in the absence of RepD gave a K_d for PcrA of 170 nM, when measured by anisotropy (Toseland, C., and Webb, M. R., unpublished results). Measurement of K_d for dT₁₀ for these conditions, but obtained as previously described (26), gave a value of 240 nM (data not shown). This suggests that RepD may increase the affinity of PcrA for DNA by an order of magnitude.

Kinetics of Formation of the RepD Complex. Two types of measurement were done to examine RepD nicking under the conditions of subsequent translocation and ATPase measurements. Data with high time resolution could be obtained using oligonucleotides, labeled with fluorescein, so that stopped-flow measurements could be made. In one set of kinetic

measurements, fluorescence anisotropy was measured following rapid mixing of RepD with Junction 3, in which the fluorescein is attached at the 5'-end of the ICRII arm rather than the end of the duplex. The traces (Figure 4a) show a rapid rise in anisotropy followed by a slow decrease to a level below that of the initial DNA. This would be expected from rapid association of the protein, then slower nicking of the ICRII, which releases the four-base oligonucleotide containing the fluorescein. Changing the RepD concentration increased the rate of the first phase but had little effect on the second (Figure 4c). Thus, the nicking rate constant for this DNA junction is 1.0 s^{-1} . This is consistent with the time limit obtained with the plasmid substrate.

In practice, the biphasic nature of these traces and small signal amplitudes made full analysis difficult, in particular obtaining accurate rate information for the first phase. To overcome this, experiments were repeated using similar experimental conditions as those described above, but rapidly mixing Junction 1 with excess RepD and measuring fluorescence intensity (Figure 4b). In this case, there is little or no signal due to nicking, and there is a single, small decrease presumably due to the initial noncovalent binding. The rate constant for this binding increases linearly with RepD concentration (Figure 4c), allowing the second order association rate constant to be determined as $1.1 \times 10^8 \text{ M}^{-1} \text{ s}^{-1}$ for this junction.

Nicking activity was validated using ion-exchange HPLC to separate the nicked 4-base product from the 45-base substrate oligonucleotide. This provides a quantitative measure of nicking in support of the fluorescence anisotropy kinetic assay outlined above. The reaction was incubated for 60 s, and after this time, only 10% of the fluorescence eluted at the position of the 45 base oligonucleotide, thus indicating a high degree of nicked oligonucleotide (data not shown).

Kinetics of Initial DNA Unwinding. A fluorometric assay was used to observe unwinding of partial duplex DNA substrates by PcrA helicase and RepD in real time. Partial duplexes of DNA, labeled with adjacent 5'-Cy3 and 3'-Dabcyl groups at the end of the duplex away from the single-stranded region, were used to measure strand separation (Junctions 4 and 5, Figure 2). In this duplex state, the fluorescence of the Cy3 dye is quenched by ~ 40 -fold by interaction with the Dabcyl moiety. This system has previously been shown to provide sufficient signal to measure duplex separation (27). At the end of the process of duplex unwinding by PcrA, Cy3 is separated from the Dabcyl quencher, and an increase in fluorescence intensity is observed. This reaction was followed on a millisecond time scale using stopped-flow fluorescence, mixing ATP rapidly with the preformed RepD-DNA-PcrA complex.

Partial duplexes without the ICRIII sequence (Junction 4, Figure 2) were used, in order to mimic the steady state of PcrA translocation during plasmid unwinding, once it is past the specific *ori* sequence. These oligonucleotide junctions have no specific sequence elements in the duplex and thus avoid any complications due to secondary structure in the inverted repeat. In the absence of RepD, PcrA was unable to unwind a duplex of 30 base pairs (Figure 5a). In the presence of RepD, there was a lag phase, followed by a rapid increase in fluorescence. PcrA moves through the duplex during the lag phase, and upon reaching the end of the duplex, the oligonucleotides separate, and the Cy3 fluorescence intensity increases. Following the initial increase in fluorescence intensity, there is a slower further increase due to PcrA dissociating, then binding and unwinding other RepD-DNA complexes in a steady state. If a large excess of dT_{50} is

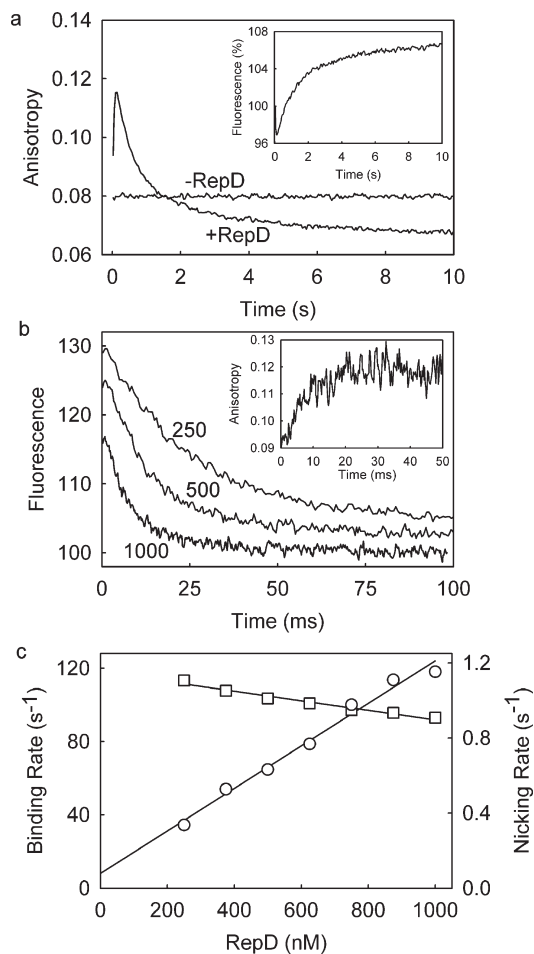


FIGURE 4: Association and nicking kinetics of RepD with a DNA junction substrate. (a) Fluorescence anisotropy following rapid mixing of 875 nM RepD with 100 nM Junction 3. The second, decay phase was fitted to a single exponential. The inset shows the equivalent fluorescence intensity trace. There was a small very slow, third phase that was not analyzed in detail. (b) Fluorescence intensity measurements were recorded, when various nanomolar concentrations of RepD, as shown, were mixed with 100 nM Junction 1. Traces were fitted to a single exponential and are offset for clarity. The inset shows a short time trace of the anisotropy for conditions as in panel a. (c) The observed rate constants from intensity traces (first phase, circles) and anisotropy (second phase, squares) were plotted against concentration for the average of two independent sets of each measurement. The slope of the linear dependence of the intensity traces (circles) gives the rate constant for RepD binding as $1.1 \times 10^8 \text{ M}^{-1} \text{ s}^{-1}$. The anisotropy slow phase represents nicking, and its rate varied only slightly with concentration. It is likely that this variation is an artifact due to fitting the middle phase of the rather noisy data. Solution conditions for both experiments were as described in Figure 3. Excitation wavelength was 497 nm, and 515 nm cutoff filters were used on the emission.

included in the ATP solution, it acts as a trap for PcrA after it dissociates from the fluorescent DNA and thus prevents binding to further substrate fluorescent DNA. This addition results in elimination of the steady-state phase to ensure that only a single turnover is observed with respect to DNA. These data indicate that RepD has a major effect on the ability of PcrA to unwind duplex DNA.

Inclusion of the ICRIII sequence in the duplex region (Junction 5, Figure 2) also resulted in RepD-dependent unwinding (Figure 5b). The kinetics were similar in the two cases, but the intensity was reduced, when compared to that in substrates without ICRIII. This reduced amplitude could be due to a

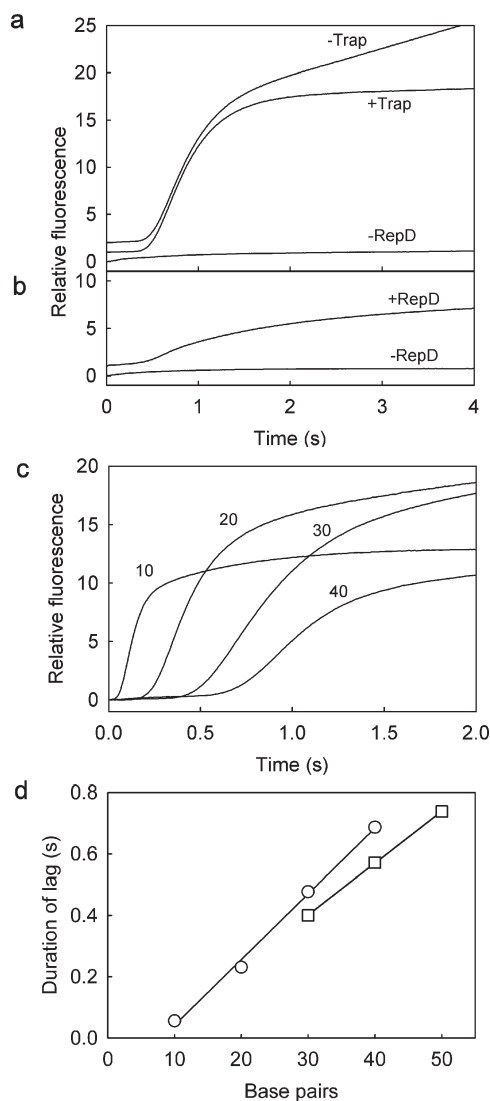


FIGURE 5: Kinetics of RepD mediated unwinding of partial duplex DNA substrates, using Cy3 fluorescence. Reactions were initiated by rapid mixing in a stopped-flow instrument. Solution conditions were the same as those in Figure 3. Cy3 was excited at 548 nm, with a 570 nm cutoff filter on the emission. Final concentrations of the mixed solution were 500 nM DNA, 2.5 μ M RepD, 95 nM PcrA, 200 μ M ATP, and ± 10 μ M oligonucleotide dT₅₀. (a) Unwinding of a 30 bp Cy3- and Dabcyl-labeled junction 4 without ICRIII (shown in Figure 2). RepD was premixed for 2 min with the DNA and then PcrA added, followed by a further 5 min of incubation. This was then rapidly mixed with ATP, which was with or without dT₅₀ to trap free PcrA. A control with no RepD or trap shows no fluorescence change. Traces are offset from each other by 1 unit on the ordinate. (b) Unwinding of a 30 bp partial duplex DNA substrate containing ICRIII (junction 5). Traces are offset from each other by 1 unit on the ordinate. (c) Unwinding of 4 lengths of DNA (without ICRIII). The duplex lengths (bp) are shown. (d) Dependence of the lag time on length of the duplex arm for data duplex without ICRIII from panel c (circles) and with ICRIII (squares). The lines are best linear fits to the average of two data sets and give rates of 47 bp s⁻¹ without ICRIII and 59 bp s⁻¹ with ICRIII.

second RepD dimer binding at ICRIII or secondary structure formation, either affecting the Cy3 and Dabcyl interaction during unwinding or reducing the loading of this oligonucleotide structure by the proteins, or reducing processivity.

Duplexes of different lengths were then used to determine the speed of unwinding of DNA substrates, i.e., translocation along the duplex. Measuring the dependence of the fluorescence change

on length potentially circumvents problems in interpretation due to end-effects in a single DNA structure. This type of measurement is better suited to short duplexes. In the absence of ICRIII, there is a change in duration of the lag phase (Figure 5c). The presence of ICRIII produced poorer data (not shown), both because of the lower amplitudes and because the presence of ICRIII means that these oligonucleotides were longer than in its absence. Thus, the analyses to obtain the lag time were not as good as that in the absence of ICRIII. Regardless of the inclusion of the ICRIII sequence, the duration of the lag phase increases linearly with the length of the DNA duplex (Figure 5d). The slope of linear fits to these data give an estimate of the unwinding rate as 47 bp s⁻¹ without ICRIII and 59 bp s⁻¹ with ICRIII. This possible difference in observed unwinding rates is addressed in the Discussion, along with the apparent intercept, suggesting no lag occurs with an ~ 8 bp length of duplex. This would, therefore, represent the minimum length of dsDNA that can be separated in this way.

In Figure 5c, the amplitude is seen to vary for the different lengths, and this may be due to several causes. The 10 bp duplex may be too short to form the initiation complex efficiently, resulting in only a fraction of the DNA unwound from time zero. In practice, the labeling efficiency varies between preparations of oligonucleotides, resulting in a variation in background fluorescence (time zero) and in the likely concentration of a doubly labeled (Dabcyl plus Cy3) junction that has both proteins bound. Therefore, interpretation of relative amplitude is difficult for this type of measurement.

ATP Hydrolysis during DNA Unwinding. The fluorescent, reagentless biosensor for phosphate, MDCC-PBP (21), was used to determine the rate of ATP hydrolysis by PcrA during unwinding of partial duplex DNA in the presence of RepD. MDCC-PBP has an ~ 7 -fold fluorescence increase upon binding inorganic phosphate (P_i), and under the conditions of these experiments, this P_i binding is rapid and quantitatively reflects the P_i produced by ATP hydrolysis. The PcrA concentration was reduced relative to the unwinding measurements, above, to ensure that the phosphate production did not saturate the sensor protein within the time period of interest. Stopped-flow fluorescence measurements were performed using unlabeled partial duplex substrates containing the right arm of ICRII, without the duplex ICRIII sequence (Junction 6, Figure 2). Figure 6 shows the P_i released during the unwinding of partial duplexes of 10, 20, 30, and 40 bp in length. For all duplex lengths, the initial rate of phosphate release is similar, with an average of 41 s⁻¹ during the first 100 ms. These initial rates represent ATP hydrolysis during unwinding. For the 10 and 20 bp duplexes, a slower second phase of phosphate release is observed, which represents multiple cycles of unwinding in a steady state. That is, the PcrA dissociates from fully separated DNA and rebinds to fresh substrate duplex. The longer duplexes do not show a clear distinction between rapid and steady-state phases, presumably because the large amount of ssDNA product represents more binding sites for PcrA and therefore increasing the steady state rate.

Equivalent measurements using oligonucleotide models that include ICRIII were not done because of the low intensity of the translocation measurements above. This presumably means that only a fraction of complexes translocate efficiently, and this would make the results ambiguous.

Kinetics of Plasmid Unwinding. A fluorometric assay was used to measure the unwinding of plasmids by PcrA in the

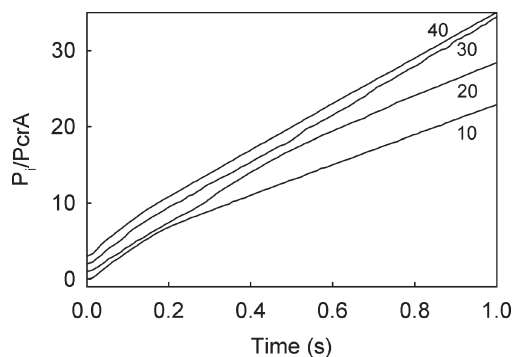


FIGURE 6: ATP hydrolysis by PcrA during unwinding of partial duplex substrates, measured using MDCC-PBP. Solution conditions were the same as those in Figure 3. MDCC-PBP was used to measure P_i formation following rapid mixing in a stopped-flow instrument. MDCC-PBP was excited at 436 nm, with a 455 nm cutoff filter on the emission. RepD was added to the solution containing DNA Junction 6 without ICRIII (Figure 2) and other lengths of duplex. It was left for 2 min prior to adding PcrA. The solutions were left for a further 5 min before being rapidly mixing with ATP with both solutions containing MDCC-PBP so that the final concentrations were 500 nM DNA, 2.5 μ M RepD, 19 nM PcrA, 200 μ M ATP, 10 μ M MDCC-PBP, 150 μ M 7-methylguanosine, and 0.1 U mL⁻¹ purine nucleoside phosphorylase. The system was calibrated using solutions of known inorganic phosphate concentration (0, 1, 2, and 3 μ M) with 10 μ M MDCC-PBP. Traces are shown, offset from each other by 2 units on the ordinate. The initial rates over 100 ms from 2 measurements for each duplex length were averaged to give an ATPase rate of 41 s⁻¹.

presence of RepD in real time (Figure 7). Single-stranded DNA binding protein, labeled with a fluorescent coumarin (DCC-SSB), was used to detect newly unwound single-stranded DNA in real time (19). This protein binds tightly and rapidly to ssDNA and gives an ~6-fold fluorescence increase on binding. For these measurements, the preformed RepD-DNA·PcrA complex was mixed with ATP in the presence of DCC-SSB. The ATP enables PcrA to start duplex separation, and the SSB then binds to the resultant ssDNA strands.

In this experiment, different concentrations of RepD and DNA were used, compared to the that in the oligonucleotide measurements, because of the different method of measurement. In this case, the signal comes from multiple fluorophores for each plasmid so that a low plasmid concentration can be used, with sufficient RepD to load the DNA fully, on the basis of the amplitude of the subsequent signal at different concentrations (data not shown). This apparently tighter affinity of RepD for the closed circular plasmid is considered in the Discussion section.

Unwinding traces show a lag phase, followed by an increase in fluorescence during unwinding, and then a final phase with slower fluorescence increase (Figure 7). The lag phase is likely to be due to several factors, such as incomplete formation of the active complex prior to mixing with ATP or initial competition for newly exposed single-stranded DNA between the labeled SSB and free PcrA in solution. The fluorescence then increases almost linearly until the plasmid is fully unwound. The last, slow increase phase can be attributed possibly to aggregation between SSB tetramers on the unwound plasmids or other slow changes that have a small effect on the fluorescence. Aggregation of SSB on unwound plasmid DNA has been imaged previously (28). The shape of the fluorescence curve was shown to be unaffected by altering the concentration of DCC-SSB between 100 and 400 nM using the 3094 bp plasmid (data not shown). Therefore, under the conditions of the measurements described here, the rate of the

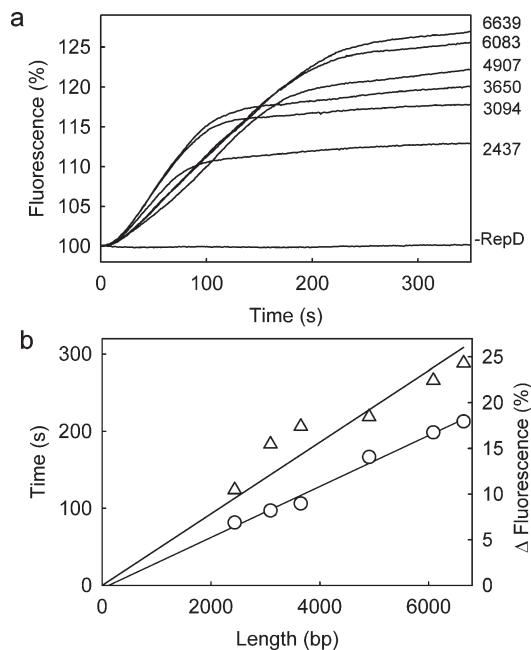


FIGURE 7: Kinetics of plasmid unwinding by PcrA and RepD, using DCC-SSB to measure the formation of ssDNA. (a) Fluorescence data for unwinding 6 plasmid lengths. Solution conditions at 30 °C were 50 mM Tris·HCl at pH 7.5, 100 mM KCl, 10 mM MgCl₂, and 1 mM EDTA. RepD was added to the solution containing the plasmid and left for 30 s before PcrA was added, and the solution was left a further 30 s before the reaction was initiated by rapid mixing of this solution, containing DCC-SSB, with ATP in a stopped-flow apparatus. Final conditions after mixing were 0.5 nM plasmid (various sizes with lengths shown in bp), 95 nM PcrA, 2 nM RepD, 200 nM DCC-SSB tetramers, and 1 mM ATP. DCC-SSB was excited at 436 nm, with a 455 nm cutoff filter on the emission. (b) Dependence of unwinding duration (circles) and amplitude (triangles) on the size of plasmid. Traces were analyzed by linear fits to fluorescence increase phases and to final phases. The amplitude and duration of unwinding were determined from the calculation of the intercept of the two fits. Two separate measurements were made for each plasmid length. The linear fit to the unwinding times gives a rate of 30 bp s⁻¹.

fluorescence increase is limited by the helicase activity separating the duplex, rather than DCC-SSB binding.

The experiment was repeated with plasmids constructed of different lengths, but each containing the same *oriD* sequence. In this way, the length dependence of unwinding is used to circumvent any end effects that may occur in analysis at a single length. The duration of the unwinding phase depends linearly on the length of the plasmid (Figure 7b). The slope of the linear fit to these data gives an unwinding rate of 30 bp s⁻¹. The amplitude of the fluorescence change also increases linearly with the size of the plasmid (Figure 7b), as the larger plasmids have a higher concentration of single stranded DNA than the smaller plasmids once unwinding has been completed. However, a number of factors may complicate this assessment of amplitudes, and these will be addressed in the Discussion section. The linearity of the time dependence for different lengths suggests that in all cases the complete plasmid is unwound.

Similar measurements, but with plasmids cut at restriction sites, gave much lower fluorescence intensity changes, in agreement with previous data (28). For example, the intact, 3094-bp plasmid gave an ~3-fold greater amplitude signal than the equivalent plasmid, cut with *Hind*III to give a 3064-bp track (data not shown). This is possibly due to lower loading by RepD, in turn due to a loss of supercoiling.

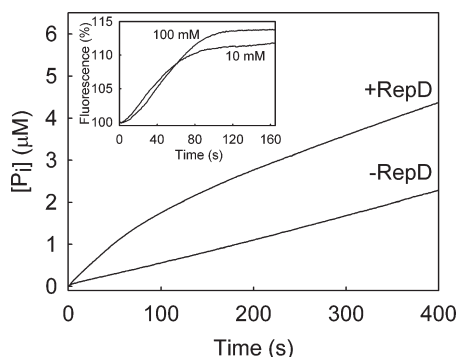


FIGURE 8: Kinetics of ATP hydrolysis during unwinding of a 3094 bp plasmid by PcrA and RepD. Solution conditions at 30 °C were 50 mM Tris·HCl at pH 7.5, 10 mM KCl, 10 mM MgCl₂, and 1 mM EDTA. RepD was added to the solution containing the plasmid and left for 30 s before PcrA was added, and the solution was left a further 30 s before the reaction was initiated by rapid mixing of this solution, containing MDCC-PBP, with ATP and heparin in a stopped-flow apparatus. Final conditions after mixing were 0.5 nM plasmid, 47 nM PcrA, ± 2 nM RepD, 20 μM MDCC-PBP, 8 mg/mL heparin, and 1 mM ATP. MDCC-PBP was excited at 436 nm, with a 455 nm cutoff filter on the emission. The system was calibrated using solutions of known inorganic phosphate concentration (0, 2, and 4 μM) in the presence of heparin. Linear fits for both traces over the first 50 s give rates of 20.5 nM P_i s⁻¹ in the presence of RepD and 5.4 nM P_i s⁻¹ in the absence of RepD. Subtracting the background rate (-RepD) from the rate with RepD and given the plasmid concentration of 0.5 nM, the active PcrA unwinding rate is 30 s⁻¹. The average from two separate measurements is 26 s⁻¹.

ATP Hydrolysis during Plasmid Unwinding. The phosphate biosensor, MDCC-PBP, was used to measure ATP hydrolysis by PcrA during plasmid unwinding (Figure 8). These measurements are complicated by the formation of bare ssDNA as product, which provides a good substrate for PcrA. SSB was not effective as a trap for free ssDNA. SSB tetramers can bind 35–70 base lengths of ssDNA but do not bind short DNA efficiently. However, PcrA, once released from the plasmid that it has unwound, presumably can bind much shorter sections of ssDNA than SSB and thereby produce rapid ATP hydrolysis. Heparin is ineffective at trapping PcrA rapidly at high ionic strength but has been shown to be effective with a related helicase at low salt (29). Therefore, heparin was used as a trap for free PcrA in low salt conditions to ensure that the phosphate produced by the active unwinding PcrA was detected and that subsequent steady state hydrolysis is minimized. As heparin also binds SSB, it was not possible to use both traps simultaneously.

In order to assess how reducing the salt concentration affects plasmid unwinding, the DCC-SSB assay was repeated at low salt (Figure 8, inset). The lag is shorter, although the main fluorescence increase has a slope similar to a somewhat lower final fluorescence level. The shorter lag in low salt may reflect, in part, the fact that SSB binding shorter lengths of ssDNA (35 bases) may predominate initially. Measurements of DNA binding to DCC-SSB suggest that at low salt, the fluorescence change is ~75% that at high salt (19). This would mean that the amplitude in terms of ssDNA is unaltered. This reduction in ionic strength caused no measurable effect on the steady-state ATPase activity of PcrA in the presence of ssDNA (data not shown). We therefore conclude that salt has only minor effects on PcrA/RepD unwinding.

For the 3094 bp plasmid in the absence of RepD, a significant background ATP hydrolysis is detected (Figure 8), suggesting that trapping by heparin is only partially successful. In the

presence of RepD, an initial rapid phase of ATP hydrolysis is observed, which slows to match the background rate after ~100 s. To calculate the rate constant for ATP hydrolysis from the active PcrA, the background rate is subtracted from this rate to give 26 s⁻¹. Unwinding data, described above, indicate that it takes ~100 s to unwind a 3094 bp plasmid, in good agreement with the ATPase activity measurement. Approximately 1 μM P_i is produced during this process. The implications of these data will be addressed in the Discussion section.

DISCUSSION

Oligonucleotide DNA substrates are capable of forming tight complexes with RepD and PcrA. Anisotropy titrations, using fluorescent DNA junctions, allowed us to assess the apparent dissociation constants, K_{app} , and showed that the presence of the ICRIII sequence increased the affinity of RepD for the DNA by ~50-fold, relative to a similar structure with ICRIII replaced by random sequence. The affinities of RepD for DNA substrates containing ICRIII and ICRII, determined here, are consistent with previous measurements (17). Currently, it is not clear whether the sequence alone or also structural elements as a result of the inverted complementary repeat is responsible for this RepD binding. However, it does suggest that the formation of the new covalent bond alone is insufficient to form the complex quantitatively. Thus, the DNA–tyrosine exchange reaction is a replacement of one phosphodiester bond by another, and the difference in bond energies is likely to be small. Indeed, the plasmid apparently forms the RepD complex more easily than either the oligonucleotide junction or, more directly comparable, the pre-cut plasmid. Possibly, release of the free energy of supercoiling in the intact plasmid, is sufficient to push the equilibrium toward complete complex formation. Once the plasmid is nicked, there is slow reversal, presumably with release of RepD and thus forming a relaxed, closed plasmid. This would also explain why the linearized plasmids might have lower loading by RepD, leading to lower amplitude of unwinding as measured by DCC-SSB (data not shown).

Rapid-reaction techniques were used to examine the details of RepD nicking. These not only provide a time framework for subsequent translocation measurements but also provide a basic mechanism for nicking. Initial RepD binding is rapid at $1.1 \times 10^8 \text{ M}^{-1} \text{ s}^{-1}$, close to diffusion control. The anisotropy measurement of nicking kinetics (1.0 s^{-1}) presumably is due to dissociation of the nicked, fluorescent, 4-base oligonucleotide and is unlikely to distinguish between this and the chemical step. The binding rate, in particular, may be influenced by the exact nature of the DNA substrate, whether plasmid or junction, or completely dsDNA. However, the nicking kinetics, both chemistry and other steps such as dissociation, are less likely to vary between DNA structures. It should be emphasized that the forked oligonucleotide substrates, used here, represent an intermediate structure during the initiation process, between the double-stranded intact *oriD* and the fully loaded initiation complex.

The addition of PcrA to a preformed complex of RepD and the DNA junction with a 10-base length of ssDNA was also quantified, and the dissociation constant of PcrA binding to RepD-loaded DNA is 22 nM (Figure 3b). This is an order of magnitude tighter than PcrA binding in the absence of RepD. Measurement of these affinities enabled suitable conditions to be chosen for subsequent unwinding experiments. In addition, the data suggest that at least part of the increased processivity of

PcrA, induced by RepD, is due to this increased affinity, potentially with a decrease in the dissociation rate of PcrA from the DNA. Processivity depends in part on the balance between the translocation rate of a helicase and its dissociation rate. The increased affinity could be due to direct interaction of RepD with PcrA, or in principle, it could be due to PcrA being bound in such a way that dissociation is physically blocked.

The data for oligonucleotide substrate unwinding (Figure 5) demonstrate that this activity of PcrA is insignificant in the absence of RepD. The oligonucleotide junctions, once loaded with RepD have only a 10 base 3'-tail of single-stranded DNA, which is unlikely to accommodate more than one PcrA molecule. Thus, in this case, it is unlikely that processive unwinding can be obtained solely by binding multiple PcrA molecules, as outlined in the Introduction section. However, our data cannot preclude the possibility that there is local unwinding, possibly associated with RepD binding, which reveals a longer stretch of ssDNA and therefore would allow a second PcrA to bind. Conditions of the measurement would be likely to preclude or at least minimize this possibility as PcrA is present at a lower concentration than the junction. With RepD bound on these oligonucleotide junctions, there is an average unwinding rate of 47 bp s^{-1} , on the basis of the length dependence of the fluorescence time course using Cy3/Dabcyl labeling. These measurements are a severe test of low processivity, as the duplex region consists of tens of base pairs, unlike the thousands in the plasmid substrates.

One feature of the plot of the lag time as a function of length in Figure 5 is that the intercept with the abscissa is at $\sim 8 \text{ bp}$, suggesting that there is no translocation when the duplex is this long. This may be due to partial unwinding of the duplex prior to the addition of ATP (equivalent to zero time), potentially as a result of PcrA interacting with RepD or just by thermal fraying. Another possible explanation is that the PcrA·RepD complex causes Cy3·Dabcyl interactions to diminish and hence Cy3 fluorescence to increase, a few bases before complete duplex separation. In contrast, equivalent experiments to measure translocation of RecG helicase (27) produce an intercept close to the origin for time versus length. This may reflect the fact that there are quite different mechanisms for these two helicases from different families. It is possible that RepD translocates along the DNA ahead of PcrA and therefore will reach the duplex end prior to complete unwinding. This provides a potential mechanism for protein interaction with the fluorophore–quencher pair a few bases before PcrA.

The ATPase data (Figure 6) show a rate of 41 s^{-1} , indicating that PcrA is likely to use one ATP for each base pair separated, considering the 47 bp s^{-1} unwinding rate determined above. This is the same coupling ratio found for PcrA translocation along a single-stranded oligonucleotide track (1). Interpretation of these ATPase data from the RepD experiments has two uncertainties. First, the bare ssDNA product of duplex separation is an excellent track for PcrA and therefore results in a high ATPase activity continuing after the duplex is separated. Second, there is a possibility that the RepD-DNA·PcrA complex is not formed quantitatively, although the titration data in Figure 3 suggest that at these concentrations the majority of PcrA molecules should be bound to a RepD-DNA complex. These limitations do not apply to the translocation (Cy3) measurement since those analyses depend only on the length dependence of the lag time. For plasmid lengths of unwinding, discussed below, the data also support a value of one ATP per base translocation.

Because of the continuing high ATPase activity after duplex separation, it is difficult to extract information directly about the amplitude of the ATP hydrolysis during the initial translocation phase. This contrasts with the situation obtained with PcrA translocation along ssDNA. In those traces, the rapid ATP usage during translocation is followed by a significant drop in rate so that the translocation phase is easily extracted from ATPase data (1). Attempts to trap PcrA in these dsDNA experiments using heparin were not successful, presumably because of the higher concentration of DNA compared with that in the plasmid unwinding experiments. In the measurements shown in Figure 6, only in the case of the 10 bp duplex is there a significant fast phase followed by a reduction in rate.

Inclusion of ICRIII in the duplex region of the oligonucleotide substrate caused a reduction in the amplitude of the unwinding signal but leaves the length of the lag very similar. Although the RepD affinity is much higher with ICRIII present, these measurements were carried out at high RepD concentration; therefore, in either case the DNA should be fully bound with RepD. The result therefore suggests that ICRIII has little or no effect on the rate for protein complexes that translocate through it but that there is a reduction in the proportion of complexes that are separated. It is possible that either RepD binding to ICRIII per se or sequence-specific effects, controlled by ICRIII, has an effect in this assay of reducing the processivity; therefore, the lag, equivalent to those in Figure 5b, would represent the shortest unwinding time in a complex process.

The data for kilobase length plasmids also show rates of 30 bp s^{-1} for unwinding and 26 s^{-1} for ATP hydrolysis. The data clearly indicate that PcrA maintains a coupling ratio of 1 ATP per base pair. The rate of 30 s^{-1} (30°C) is significantly less than the rate of 50 s^{-1} (20°C) observed for translocation along single-stranded oligonucleotide substrates.

The data obtained for unwinding plasmid-length DNA provide evidence that a single PcrA·RepD complex has large enough processivity to unwind a complete plasmid and does it with tight coupling of 3' to 5'-translocation with ATP hydrolysis. For the 3094 bp plasmid, the unwinding time taken from Figure 7 is $\sim 100 \text{ s}$, and the amount of ATP hydrolyzed in this time is only slightly less than expected, if 100% of the plasmid were unwound by a single PcrA monomer. Because there is a heparin trap for free PcrA, premature dissociation of PcrA from a partially unwound plasmid would cause a reduction in yield of P_i . The equivalent trapping experiment could not be performed, when using the SSB fluorescence probe, as heparin binds to SSB. Attempts to trap with dT₅, potentially long enough to trap PcrA but too short for effective SSB binding, were not effective. This suggests that a single PcrA, once recruited by RepD to the dso, largely remains bound until the plasmid is fully unwound, although we cannot completely exclude the possibility of PcrA dissociating then rapidly re-binding prior to any re-annealing.

Data, reported in this study, agree with previous studies in that RepD has a large effect on the ability of PcrA to unwind DNA (2, 28). We have demonstrated that PcrA on its own is unable to unwind DNA substrates as short as 30 bp, yet in the presence of RepD a single PcrA molecule can unwind a plasmid of over 6 kb. A previous study (30) on a related helicase, Rep, showed that an increase in apparent unwinding activity occurred by deleting a particular domain (2B) of that helicase. It is possible that RepD may act to increase helicase activity via a protein–protein interaction within this domain of PcrA.

Considering the biological implications of these data, the rates of unwinding would equate to 2–3 min for complete separation of the 4.6 kb natural plasmid, pC221, at 30 °C. Assuming that this process is limiting in the plasmid replication, the leading strand synthesis of pC221 would also take this time. Previous studies have demonstrated from incorporation of radioactively labeled nucleotide into cell extracts from a closely related system (pT181) that significant amounts of supercoiled product are formed and that one round of replication may occur within 10 min (31). DNA polymerase may well play an active role in helicase activity as well as in its specific role of replicating the circular, leading strand DNA exposed by PcrA and RepD. DNA polymerase III holoenzyme from *S. aureus* has been reported to synthesize DNA at a rate of ~700 nucleotides s⁻¹ *in vitro* at 37 °C (32), which is significantly faster than the rates reported in this study. The source of the PcrA used here is not *S. aureus*, and this may cause suboptimal interactions. The polymerase may increase unwinding rates by pushing PcrA; however, PcrA translocation may reduce the rate of DNA polymerase. In either case, it seems likely that unwinding and synthesis occur at similar rates.

ACKNOWLEDGMENT

We thank Mrs. J. Hunter (NIMR, London) for preparing MDCC-PBP and Ms. K. Tibbles and Mr. A. Chavda (NIMR, London) for preparing DCC-SSB.

REFERENCES

- Dillingham, M. S., Wigley, D. B., and Webb, M. R. (2000) Demonstration of unidirectional single-stranded DNA translocation by PcrA helicase: measurement of step size and translocation speed. *Biochemistry* 39, 205–212.
- Soultanas, P., Dillingham, M. S., Papadopoulos, F., Phillips, S. E., Thomas, C. D., and Wigley, D. B. (1999) Plasmid replication initiator protein RepD increases the processivity of PcrA DNA helicase. *Nucleic Acids Res.* 27, 1421–1428.
- Niedziela-Majka, A., Chesnik, M. A., Tomko, E. J., and Lohman, T. M. (2007) *Bacillus stearothermophilus* PcrA monomer is a single-stranded DNA translocase but not a processive helicase *in vitro*. *J. Biol. Chem.* 282, 27076–27085.
- Velankar, S. S., Soultanas, P., Dillingham, M. S., Subramanya, H. S., and Wigley, D. B. (1999) Crystal structures of complexes of PcrA DNA helicase with a DNA substrate indicate an inchworm mechanism. *Cell* 97, 75–84.
- Subramanya, H. S., Bird, L. E., Brannigan, J. A., and Wigley, D. B. (1996) Crystal structure of DExx box DNA helicase. *Nature* 384, 379–383.
- Dillingham, M. S., Soultanas, P., Wiley, P., Webb, M. R., and Wigley, D. B. (2001) Defining the roles of individual residues in the single-stranded DNA binding site of PcrA helicase. *Proc. Natl. Acad. Sci. U.S.A.* 98, 8381–8387.
- Yang, Y., Dou, S.-X., Ren, H., Wang, P.-Y., Zhang, X.-D., Qian, M., Pan, B.-Y., and Xi, X. G. (2008) Evidence for a functional dimeric form of the PcrA helicase in DNA unwinding. *Nucleic Acids Res.* 36, 1976–1989.
- Bird, L. E., Brannigan, J. A., Subramanya, H. S., and Wigley, D. B. (1998) Characterisation of *Bacillus stearothermophilus* PcrA helicase: evidence against an active rolling mechanism. *Nucleic Acids Res.* 26, 2686–2693.
- Levin, M. K., Wang, Y. H., and Patel, S. S. (2004) The functional interaction of the hepatitis C virus helicase molecules is responsible for unwinding processivity. *J. Biol. Chem.* 279, 26005–26012.
- Byrd, A. K., and Raney, K. D. (2005) Increasing the length of the single-stranded overhang enhances unwinding of duplex DNA by bacteriophage T4 Dda helicase. *Biochemistry* 44, 12990–12997.
- Iordanescu, S., and Bargonetti, J. (1989) *Staphylococcus aureus* chromosomal mutations that decrease efficiency of Rep utilization in replication of pT181 and related plasmids. *J. Bacteriol.* 171, 4501–4503.
- Khan, S. A. (1997) Rolling-circle replication of bacterial plasmids. *Microbiol. Mol. Biol. Rev.* 61, 442–455.
- Gennaro, M. L., Iordanescu, S., Novick, R. P., Murray, R. W., Steck, T. R., and Khan, S. A. (1989) Functional organization of the plasmid pT181 replication origin. *J. Mol. Biol.* 205, 355–362.
- Noirot, P., Bargonetti, J., and Novick, R. P. (1990) Initiation of rolling-circle replication in pT181 plasmid: initiator protein enhances cruciform extrusion at the origin. *Proc. Natl. Acad. Sci. U.S.A.* 87, 8560–8564.
- Thomas, C. D., Balson, D. F., and Shaw, W. V. (1990) *In vitro* studies of the initiation of Staphylococcal plasmid replication. Specificity of RepD for its origin (*oriD*) and characterization of the RepD-*ori* tyrosyl ester intermediate. *J. Biol. Chem.* 265, 5519–5530.
- Projan, S. J., Kornblum, J., Moghazeh, S. L., Edelman, I., Gennaro, M. L., and Novick, R. P. (1985) Comparative sequence and functional analysis of pT181 and pC221, cognate plasmid replicons from *Staphylococcus aureus*. *Mol. Gen. Genet.* 199, 452–464.
- Thomas, C. D., Nikiforov, T. T., Connolly, B. A., and Shaw, W. V. (1995) Determination of sequence specificity between a plasmid replication initiator protein and the origin of replication. *J. Mol. Biol.* 254, 381–391.
- Pace, C. N., Vajdos, F., Fee, L., Grimsley, G., and Gray, T. (1995) How to measure and predict the molar absorption coefficient of a protein. *Protein Sci.* 4, 2411–2423.
- Dillingham, M. S., Tibbles, K. L., Hunter, J. L., Bell, J. C., Kowalczykowski, S. C., and Webb, M. R. (2008) Fluorescent single-stranded DNA binding protein as a probe for sensitive, real time assays of helicase activity. *Biophys. J.* 95, 3330–3339.
- Webb, M. R. (2003) A Fluorescent Sensor to Assay Inorganic Phosphate, in *Kinetic Analysis: A Practical Approach* (Johnson, K. A., Ed.) pp 131–152, Oxford University Press, Oxford, U.K.
- Brune, M., Hunter, J. L., Howell, S. A., Martin, S. R., Hazlett, T. L., Corrie, J. E. T., and Webb, M. R. (1998) Mechanism of inorganic phosphate interaction with phosphate binding protein from *Escherichia coli*. *Biochemistry* 37, 10370–10380.
- Jacques, L. B. (1977) Determination of heparin and related sulfated mucopolysaccharides. *Methods Biochem. Anal.* 24, 203–312.
- Brownbridge, G. G., Lowe, P. N., Moore, K. J. M., Skinner, R. H., and Webb, M. R. (1993) Interaction of GTPase activating proteins (GAPs) with p21ras measured by a novel fluorescence anisotropy method. Essential role of Arg-903 of GAP in activation of GTP hydrolysis on p21ras. *J. Biol. Chem.* 268, 10914–10919.
- Leatherbarrow, R. J. (2001) *Grafit Version 5*, Erithacus Software Ltd., Horley, U.K.
- Eccleston, J. F., Hutchinson, J. P., and White, H. D. (2001) Stopped-Flow Techniques, in *Protein Ligand Interactions: Structure and Spectroscopy. A Practical Approach Series* (Harding, S. E., and Chowdry, B. Z., Eds.) pp 201–237, Oxford University Press, Oxford, U.K.
- Dillingham, M. S., Wigley, D. B., and Webb, M. R. (2002) Direct measurement of single stranded DNA translocation by PcrA helicase using the fluorescent base analogue 2-aminopurine. *Biochemistry* 41, 643–651.
- Martinez-Senac, M. M., and Webb, M. R. (2005) Mechanism of translocation and kinetics of DNA unwinding by the helicase RecG. *Biochemistry* 44, 16967–16976.
- Zhang, W., Dillingham, M. S., Thomas, C. D., Allen, S., Roberts, C. J., and Soultanas, P. (2007) Directional loading and stimulation of PcrA helicase by the replication initiator protein RepD. *J. Mol. Biol.* 371, 336–348.
- Tomko, E. J., Fischer, C. J., Niedziela-Majka, A., and Lohman, T. M. (2007) A nonuniform stepping mechanism for *E. coli* UvrD monomer translocation along single-stranded DNA. *Mol. Cell* 26, 335–347.
- Cheng, W., Brendza, K. M., Gauss, G. H., Korolev, S., Waksman, G., and Lohman, T. M. (2002) The 2B domain of the *Escherichia coli* Rep protein is not required for DNA helicase activity. *Proc. Natl. Acad. Sci. U.S.A.* 99, 16006–16011.
- Khan, S. A., Carleton, S. M., and Novick, R. P. (1981) Replication of plasmid pT181 DNA *in vitro*: requirement for a plasmid-encoded product. *Proc. Natl. Acad. Sci. U.S.A.* 78, 4902–4906.
- Bruck, I., Georgescu, R. E., and O'Donnell, M. (2005) Conserved interactions in the *Staphylococcus aureus* DNA PolC chromosome replication machine. *J. Biol. Chem.* 280, 18152–18162.